Journal Homepage: https://dergipark.org.tr/tr/pub/isibted

Isı Bilimi ve Tekniği Dergisi

Archive: https://tibtd.org.tr/dergi

Investigations on Thermal Performance of an Electronic Board using Conduction-Based Finite Element Method with a New Modeling Approach

Yener USUL [1], Şenol BAŞKAYA [2], Bülent ACAR [1], Tamer ÇALIŞIR [3,*]

[1] *Roketsan Inc. Ankara, Türkiye*
[2] *University of Kyrenia Faculty of Aviation and Space Sciences Dept. of Aeronautical Engineering, Girne, North Cyprus*
[3] *Gazi Üniversitesi Mühendislik Fakültesi Makina Mühendisliği Bölümü 06570 Maltepe, Ankara, Türkiye*

A R T I C L E I N F O

2024, vol. 44, no.2, pp. 294-307

doi: 10.47480/isibted.1563932

Research Article
Received: 18 September 2023
Accepted: 22 August 2024

* *Corresponding Author*
e-mail: tamercalisir@gazi.edu.tr

Keywords:
Conduction-based finite element method (FEM)
Experiment
Natural Convection
Thermal Management

ORCID Numbers in author order:
0000-0002-1087-4743
0000-0001-9676-4387
0000-0002-0721-0444

A B S T R A C T

Electronic systems are used in almost all areas of industry, with an increasing power consumption rate. This trend makes thermal management of electronics compulsory in order for proper operation. Several methods can be employed to examine electronics' thermal behavior. Conduction-based Finite Element Method (FEM) for heat transfer analysis is one of them; providing accurate solutions within short solution times is one of its outstanding advantages. Nevertheless, the fluid inside or around the system, usually air for electronic systems, is not included directly in the conduction-based FEM analysis model. This is an essential deficiency in terms of solution accuracy. If this drawback is overcome, conduction-based FEM will become a preferred analysis method, especially for transient problems under natural convection. In this study, a conduction-based FEM analysis model of an electronic board with two heat-dissipating components inside an enclosure under transient natural convection was developed. The procedure of the model involves the correction of unknown input parameters. An experimental investigation was performed, the results of which were used as reference values for the correction process. These unknown parameters were determined iteratively. The iteration was continued until the results of the analysis and those of the experiment matched. The difference between the results of the analysis and those of the experiment was less than 2-3°C. Some parametrical thermal investigations were performed on the electronic board using the final analysis model.

İletim Tabanlı Sonlu Elemanlar Yöntemi Kullanılarak Yeni bir Modelleme Yaklaşımı ile bir Elektronik Kartın Isıl Performansının İncelenmesi

M A K A L E B İ L G İ S İ

Anahtar Kelimeler:
İletim Tabanlı sonlu eleman yöntemi
Deney
Doğal Konveksiyon
Isıl Yönetim

Ö Z E T

Elektronik sistemler, artan güç tüketimiyle birlikte sanayinin hemen her alanında kullanılmaktadır. Bu eğilim, elektronik elemanların düzgün çalışması için termal yönetimini zorunlu kılmaktadır. Elektronik elemanların termal davranışını incelemek için çeşitli yöntemler kullanılmaktadır. Isı transferi analizi için İletim Tabanlı Sonlu Elemanlar Yöntemi (SEY) bunlardan biridir; Kısa çözüm sürelerinde doğru çözümler sunması öne çıkan avantajlarından biridir. Bununla birlikte, sistemin içindeki veya etrafındaki akışkan (elektronik sistemler için genellikle hava), doğrudan iletim tabanlı SEY analiz modeline dahil edilmez. Bu çözüm doğruluğu açısından önemli bir eksikliktir. Bu dezavantajın aşılması durumunda, iletim tabanlı SEY, özellikle doğal taşınım altındaki geçici problemler için tercih edilen bir analiz yöntemi haline gelecektir. Bu çalışmada, zamana bağlı doğal konveksiyon altında bir kapalı ortam içinde iki ısı kaynağına sahip bir elektronik kartın iletim tabanlı SEY analiz modeli geliştirilmiştir. Modelin prosedürü bilinmeyen parametrelerinin düzeltilmesini içermektedir. Sonuçları düzeltme işlemi için referans değerleri olarak kullanılan deneysel bir araştırma gerçekleştirilmiştir. Bu bilinmeyen parametreler iteratif olarak belirlenmiştir. Analiz sonuçları ile deneyin sonuçları eşleşene kadar iterasyona devam edildi. Analiz sonuçları ile deneysel sonuçlar arasındaki fark 2-3°C'nin altında olduğu tespit edilmiştir. Son analiz modeli kullanılarak elektronik kart üzerinde bazı parametrik termal incelemeler gerçekleştirilmiştir.

NOMENCLATURE

α	Thermal diffusivity (m^2/s)
C	Coefficient (-)
c_p	Specific Heat (J/kg.K)
ε	Emissivity (-)
h	Heat Transfer Coefficient ($W/m^2.K$)
k	Thermal conductivity (W/m.K)
L	Characteristic lenght (m)
Nu	Nusselt number (-)
q	Heat flux (W/m^2)
Q	Thermal power (W)
R	Thermal resistance ($m^2.k/W$)
Ra	Rayleigh number (-)
T	Temperature (°C)
$T_{heater\ plate}$	Heater plate temperature (°C)
$T_{initial}$	Initial temperature (°C)

INTRODUCTION

Electronic systems are excessively used in almost all areas of industry. Moreover, the demand for the usage of electronic systems is increasing continuously. This demand makes the macro level packaging of the electronics more compact, which causes a higher rate of heating with a lower cooling capacity. Because of this, thermal management is vital for electronic systems, especially for those placed in narrow enclosures with a high heat dissipating rate. Automobiles, airplanes, missiles, and informatics can be seen as the areas of application, where the thermal management of electronics is important.

There are two main stages in the thermal management of electronics. The first one is to take precautions during the design phase, in order to minimize the internal and external heating and to let the heat be released from the system. The second stage of thermal management is finding a solution for cooling the system. If the first stage is applied properly, the need for the second step is minimized. In this way, additional costs, weight, maintenance, etc., that come from the use of extra equipment for thermal management are minimized. Therefore, great attention should be paid to the precaution step of the electronics during the design phase, to get more economical and robust systems.

An electronic system can be analyzed experimentally and numerically in practical applications, in terms of thermal considerations. The experimental method is usually the most accurate. Nevertheless, some factors, such as cost, repeatability, accessibility, are disadvantages to experimental methods. Considering the combined effect of cost, accuracy, repeatability, etc., numerical methods are the best choice. There are different numerical methods. The most commonly used ones are CFD (Computational Fluid Dynamics) and conduction-based FEM (Finite Element Method) for the analyses of electronic systems used in practice. Since fluid inside or around the system is modeled in the CFD method, computation time can be long, especially for time-dependent conjugate heat transfer problems with natural convection behavior. On the other hand, for the conduction-based FEM, the fluid inside the computational domain is not directly included in the model. Instead, the heat transfer between the solid and the fluid part inside the computational domain is accounted for by applying a proper boundary condition. Once the conduction-based FEM model and the convective heat transfer boundary conditions are set up properly and correctly, accurate results can be obtained by solving the main disadvantage of the CFD approach, which is the long solution time for time-dependent conjugate heat transfer problems, including natural convection.

Some studies have conducted on the thermal analysis of electronic systems at different levels, such as the component level, the board level, and the system level, using different methods in the literature. Ocak (2010) studied the thermal behavior of an electronic board experimentally and numerically at different configurations. CFD analyses were performed by the author. The board and the components were modeled according to conduction-based compact thermal modeling, at five different levels. The problem includes natural convection for one configuration and forced convection for another. Eveloy and Rodgers (2005) performed a numerical and experimental study of an electronic board carrying a 160-lead PQFP (Plastic Quad Flat Pack) component. The effects of the ambient velocity, and an increasing rate of the ambient temperature were researched. The CFD analyses were performed as conjugate and segregated, and the results were compared with experimental results. Byon et al. (2011) studied the variation of the thermal performance of a chip for different chip thickness and power values. Since geometry is not complicated, the results of the experiment and the analytical solutions matched well. Lira and Greenlee (2007) performed detailed and simplified numerical thermal analyses of an electronic board. The convective heat transfer coefficients were obtained using the empirical relations in the literature. The results of the analyses were compared. The simplified model is said to be enough for data that are relatively more general. However, for the results that are more specific, such as, the temperature values of the components, a detailed modeling technique is preferred. Joshy et al. (2017) examined the thermal behavior of electronic boards placed in a parallel configuration. The examination was carried out for both steady and transient state and both experimental and numerical methods were employed. Resistor-capacitor method was used as the numerical method. Lim et al. (2021) investigated the effect of independent variables on the thermal behavior of flexible printed circuit boards in order to obtain optimum cooling performance with least deflection and stress. The optimized Reynolds number has been identified in the range of 21364-29367 for various packages. Otaki et al. (2022) described a method where they combined the Bayesian optimization and lumped-capacitance thermal network model for speeding up of the thermal design optimization of electronic circuit board layouts. Wang et al. (2024) investigated the thermal design of a PCB by using micro-pin fin array heat sinks. They investigated four different types of micro-pin fin arrays. Rakshith et al. (2022) showed an overview about the design and operation of thermal ground planes and their applications to various fields.

Thermal performance of electronics at the component level, the board level, and the system level was analyzed by conduction-based methods (Develliođlu, 2008; Cheng et al., 2013; Cheng et al., 2008; Chen et al., 2003; Zahn and Stout, 2002), for different geometrical and boundary conditions for

steady-state problems. The convective HTCs (Heat Transfer Coefficients) for those studies were calculated using empirical relations obtained from the literature.

CFD analyses were performed for electronic systems in an enclosure under natural convection to examine the effects of different geometries and boundary conditions at different levels, such as the component level, the board level, the and system level (Xu, 2017; Stancato et al., 2017; Eveloy et al., 2002). All of them were conducted for steady-state conditions, because the solution of conjugate CFD problems for heat transfer problems under transient natural convection takes long time. In the studies of Han and Jung (2017) and Rodgers et al. (1999) similar studies were carried out, by modeling some extra geometrical details.

CFD analyses, together with experimental studies, were performed for the purpose of comparison of the system level and component level electronic units (Taliyan et al., 2010; Chavan and Sathe, 2016; Pang, 2005; Rosten et al., 1995). The systems and components were inside an enclosure in the above mentioned studies. Parametric studies were performed under steady-state conditions for different values of the geometrical and boundary conditions.

There are also studies in which the thermal behavior of the air inside an enclosure was examined, with heat sources at the walls of the enclosure instead of electronic components or systems (Deng, 2008; Khatamifar et al., 2017; Zaman et al., 2013; Nogueira et al., 2011). The results of those studies can be utilized to determine the way to examine the thermal performance of electronics, since the geometry and boundary conditions resemble electronic systems.

Battula et al. (2024) investigated numerically the combined effect of conduction, convection and radiation from a heated vertical electronic board. They obtained the optimum values of surface emissivity, thermal conductivity and modified Richardson number.

Some studies mentioned above examined the thermal performance of electronic components under different geometrical and boundary conditions, by utilizing experimental or numerical methods that include CFD, conduction-based FEM, or resistor-capacitor methods. Other studies evaluated and compared the analysis methods among each other or with the experimental method. However, no study is about tuning the conduction-based FEM model parameters by using experimental data in order to improve the accuracy of the FEM without making any concessions on short solution time, by virtue of the conduction-based FEM.

This study examined the thermal performance of an electronic board with two heat-dissipating components for different boundary conditions, parametrically. Conduction-based FEM was used to examine the thermal performance of the board. Before the parametric analyses, a proper analysis model was set up. The set up process included the determination of the analysis model input parameters that were unknown or uncertain. These were: thermal contact resistance values between the components and the PCB (Printed Circuit Board), component power deration rate, which is the deration of the power of the resistor-type components after they exceeded a certain temperature, generally 75°C, and coefficients for calculating the natural convective HTCs at PCB and component surfaces. The determination of the coefficients for calculating the natural convective HTCs was the key in eliminating the main disadvantages to the conduction-based FEM.

The aims of the present study were to show a comparison of the thermal behavior of the system under various boundary conditions, and to obtain the most suitable analysis method.

PROBLEM DESCRIPTION

In this part of the study, the applied experimental and numerical model has been described. The used experimental setup and experimental procedure has been introduced. Afterwards, the numerical model has been given.

The determination of the input parameters were achieved by performing an experiment and corresponding analyses, iteratively. The results of the experiments were used as reference values. The initial analyses were performed with initial values of the input parameters. The initial values were guessed within a physically sensible range. Then, the results of the experiments and the initial analyses were compared. According to the difference between the results, the initially guessed values of the input parameters were tuned. Analyses were repeated with those tuned values, and the results were compared again with the experimental results. Parameters were updated, within a physically acceptable range. This iterative process continued until the results of the experiments and the analysis matched within an acceptable error range.

The iterative comparison was made for thermal contact resistance between the components and the PCB, component power deration rate, and the coefficient used to calculate the natural convective HTCs on the surfaces in a certain order, in order to minimize the number of unknowns. First, the thermal contact resistance values were determined. Then, the power deration rate and coefficients for calculating the convective HTC on the surfaces have been obtained. A representative flow diagram of the whole process is shown in Fig. 1.

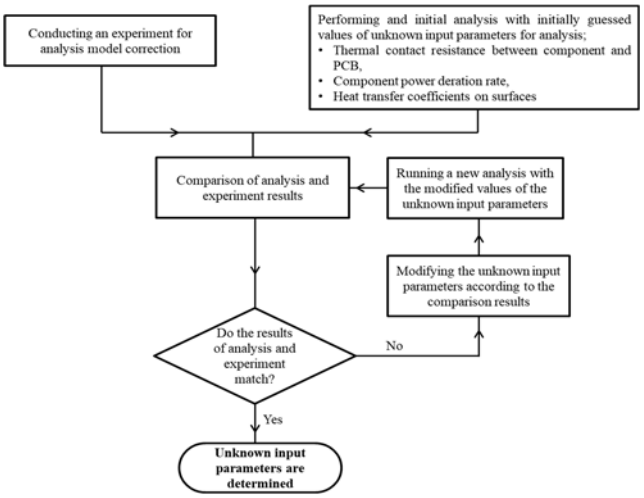

Figure 1. The flow diagram of the proposed thermal analysis model.

Experimental Setup

The experiments were conducted inside an enclosure of a size of 300 mm × 300 mm × 300 mm. The main body of the enclosure was made of aluminum. To prevent heat loss as much as possible, thermal insulation was applied outside of

the main body. There was a 290 mm × 290 mm heater plate at the bottom of the enclosure, which covers almost the whole bottom area. The purpose of the heater plate is to provide a desired temperature profile to the sample from the bottom side. There were heater resistors under the plate to supply heat to the plate. The resistors were controlled by a manual type of variac, in order to control the power supplied to the heater resistors. The input voltage to the resistors can be adjusted to any value within a continuous range of 0–220 V using the variac. A photograph of the experimental setup, the power supply, and the placement of the PCB inside the enclosure is presented in Fig 2.

Figure 2. A general view of the experimental setup.

There were thermocouples inside the heater plate to measure its temperature, in order to adjust the variac at the correct value. In addition to the embedded thermocouples, there were 10 more thermocouples for the temperature measurement of the air inside the enclosure.

Experimental Procedure

The purpose of the experiments was to obtain reference results for correction of the analysis model. The experiments were performed in a certain sequence, according to the model's correction sequence. The experiments were composed of two parts. In the first part, the heater plate was heated from room temperature to 60°C, with a heating rate of 2.8°C/min for approximately 650 seconds and then maintained at 60°C for 350 seconds. The components of the PCB were powered off during the first session of the experiments. The second part of the experiments was conducted by maintaining the heater plate at a constant temperature of 60 °C, while the components were powered on. The first part persisted for 1000 seconds, while the second part lasted for 600 seconds.

During the whole experiment, the temperature of the components and the PCB was measured via thermocouples in certain locations (S-1, S-2, and S-3), which are shown in Fig. 3.

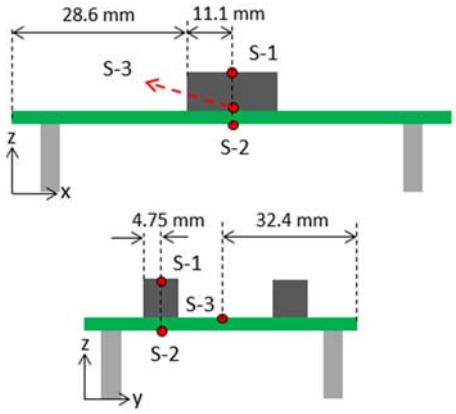

Figure 3. Locations on electronic board where temperature changes with time.

Uncertainty Analysis

An uncertainty analysis was performed to determine the accuracy of the experimental measurements. The uncertainty has been obtained according to the procedure of Holman (1994). The uncertainty of variables have been obtained by using the root-sum-square formulation:

$$W_R = \left[\left(\frac{\partial R}{\partial x_1} W_1\right)^2 + \left(\frac{\partial R}{\partial x_2} W_2\right)^2 + \left(\frac{\partial R}{\partial x_3} W_3\right)^2 + \ldots\ldots\ldots + \left(\frac{\partial R}{\partial x_n} W_n\right)^2 \right]^{1/2} \quad (1)$$

where R is the result of a given function of the independent variables x_1, x_2, x_3,...,x_n. W_R shows the uncertainty of the variable R, and $W_i(W_1, W_2,...,W_n)$ represents the uncertainty of the independent variable. The uncertainties obtained for calculated variables have been given in Table 1.

Table 1. Measurement Uncertainties.

Variable	Value	Uncertainty	Percentage Uncertainty (%)
Heat Transfer in the component	Q_{comp}=793 W	W_{Qcomp} = 0.0143	1.80
Thermal resistance along electronic board	R_{board}=0.00483 m²K/W	W_{Rboard} = 0.000167	3.45
Heat flux from the component to the electronic board by conduction	q_{cond}=627.28 W/m²	W_{qcond} = 77.04	12.30
Heat stored in the component	Q_{st}=0.49254 W	W_{Qst} = 0.0161	3.27
Heat transfer by convection and radiation from the component	$Q_{conv+Qrad}$ = 0.1681 W	$W_{Qconv+Qrad}$ = 0.0217	12.90
Experimentally obtained heat transfer coefficient	h=13.2 W/m²K	W_h = 1.756	13.30
Rayleigh number	Ra=8630	W_{Ra} = 474.7	5.50
Nusselt number	Nu=5.2	W_{Nu} = 0.0715	1.38

Numerical Model

ABAQUS, a commercial conduction-based FEM software, was used in the numerical study. The enclosure was excluded from the analysis model. In order to represent the heat transfer effects of the air on the solid parts, convective heat transfer boundary conditions were defined on the surface of the components and the PCB.

Mathematical Formulation

The numerical method used in this study contains no fluid motion. Therefore, only conduction through solid parts was

considered. The fundamental equation used for conduction-based FEM heat transfer analysis is the general heat conduction equation for three-dimensional space, given in Eq. (2):

$$\frac{\partial^2 T}{\partial x^2}+\frac{\partial^2 T}{\partial y^2}+\frac{\partial^2 T}{\partial z^2}+\frac{\dot{q}}{k}=\frac{1}{\alpha}\frac{\partial T}{\partial t} \quad (2)$$

where, T is temperature, x, y, and z are coordinate axes, is the internal heat generation, k is the thermal conductivity, α is the thermal diffusivity and t is time.

In the first part of the analysis, where the components were powered off, the heater plate was the only heat source, and it was heated from room temperature to 60°C. Convective heat transfer boundary conditions were applied on the surface of the electronic board and the components. The convective heat transfer boundary condition was defined to take the combined effects of convective and radiative heat transfer between the heater plate and the electronic board. The temperature range and temperature differences between the plate and the board were appropriate for accepting this combined boundary condition assumption. The ambient temperature was taken from the experimental data, to define the convective heat transfer boundary condition. The following equations were used for the calculation of the combined convective radiative heat transfer coefficient:

$$q_{radiative}=\varepsilon\sigma\left(T_1^4-T_2^4\right) \quad (3)$$

$$q_{radiative}=\varepsilon\sigma\left(T_1+T_2\right)\left(T_1^2+T_2^2\right)\left(T_1-T_2\right) \quad (4)$$

$$q_{radiative}=h_{equivalent}\left(T_1-T_2\right) \quad (5)$$

$$h_{equivalent}=\varepsilon\sigma\left(T_1+T_2\right)\left(T_1^2+T_2^2\right) \quad (6)$$

where, qradiative is the radiative heat transfer, hequivalent is the combined convective and radiative heat transfer coefficient, T_1 and T_2 are the surface and the environment temperatures between which the radiative and convective heat transfer occurs and ε and σ are emissivity and the Stefan-Boltzmann constant, respectively.

In the second part of the analysis, heat dissipation inside the components was defined. Radiative heat transfer between the heater plate and the electronic board was ignored, since the temperature difference between them was low enough. Heat was transferred between the plate and the electronic board by conduction and convection. The temperature values were defined at the legs of the PCB as Dirichlet boundary condition for both stages of the analysis, since the heater plate was not included in the model.

Thermal contact resistance was defined for the component and the PCB interfaces. Nevertheless, thermal contact resistance was ignored at the interface between the PCB-legs and legs-heater plate, because those parts were mounted tightly.

Mesh Independency Study for FEM

A mesh independency study was performed to determine the optimal mesh size. The temperature distribution on a path shown in Fig. 4 was used for the mesh independency study. Analyses for a dummy boundary condition were performed for mesh sizes of 5, 2.5, 1.25, and 0.625 mm.

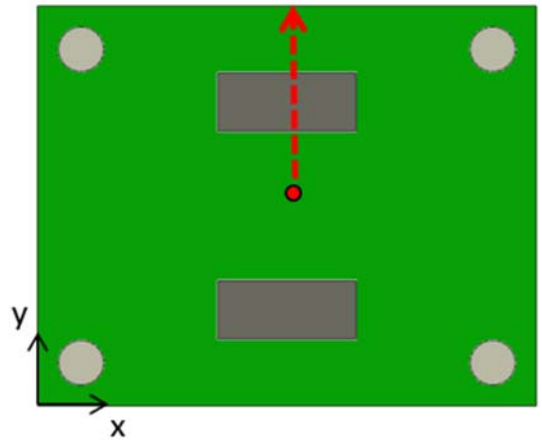

Figure 4. The path on which the temperature distribution was extracted at 600 s in conduction-based FEM analyses.

The results of the temperature distribution on the path for the predetermined mesh sizes are shown in Fig. 5. 1.25 mm and sizes lower than that are proper for accurate results, as it is seen in Fig. 5. Therefore, a 1.25 mm average mesh size was used for all analyses from this point on.

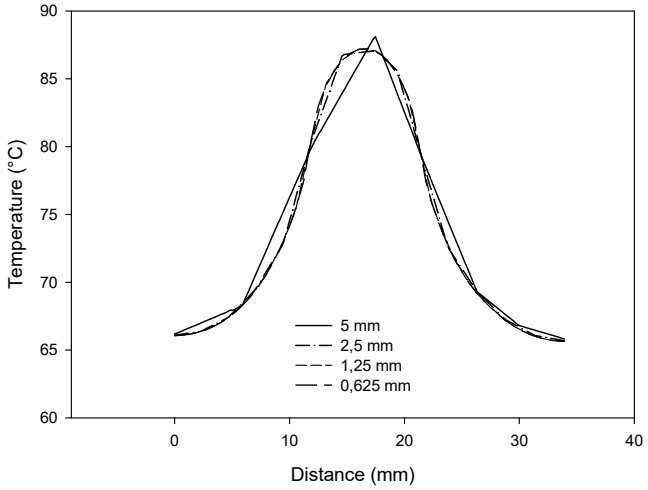

Figure 5. Temperature distribution on PCB at 600 s for different mesh sizes.

CORRECTION OF THE CONDUCTION-BASED FEM

The unknown input parameters in this study were the heat transfer coefficients on the surfaces, thermal contact resistance values between the components and the PCB, and the power generation rate of the components, occurring at high temperatures.

The determination procedure of the unknown input parameters should have been performed in an appropriate sequence, to minimize the number of unknowns at the same process. Thermal contact resistance values must be known in any case, since the heat will flow through the components and PCB interface if there is a temperature difference between the components and the PCB. The convective heat transfer coefficients were also necessary for all analyses. On the other hand, the power generation rate was necessary only when the components were powered on. Considering these phenomena, an analysis model correction had to be conducted, starting from the case where the components

were powered off. Hence, the number of unknown parameters was reduced in one of the correction steps. That is the reason why the experiments were conducted in two sessions, as mentioned before.

All of the unknown input parameters were determined by an iterative process. Initially, some values were chosen from a physically acceptable range of the unknown input parameters. Then, an initial analysis was run with the initially guessed values of the unknown input parameters. The results from the experiments and the initial analysis were compared, and the guessed values were updated according to the difference between them. This process continued until the results of the analysis and the experiment matched within an acceptable error band. The foregoing correction procedure was repeated for all unknown input parameters. This iterative procedure was performed using Isight, a commercial integrator software.

Determination of Thermal Contact Resistances

The thermal contact resistance values were determined using the first part of the experiment and the analysis, where the components were powered off. The only heat source in the system in that part was the heater plate. The outer part of the components was made of ceramic. The surface of the PCB was mid-level rough. No extra pressure was applied on the components. With these facts, a range of 1–100 m^2K/W was chosen, within which the thermal contact resistance values were changed iteratively (Gilmore and Donabedian, 2003).

Since the temperature of the system was not very high in the first part of the experiment, and there was only a small temperature gradient in the system, the heat transfer coefficient of all surfaces was taken to be 5 W/m^2K. By this assumption, the number of unknowns was reduced with a small loss in accuracy. Conduction-based thermal FEM analyses were performed for thermal contact resistance values, R, of 1, 10, and 100 m^2K/W. The results of those analyses have been presented in Fig. 6, together with experimental results for S-2 point. Only the results of the S-2 point were presented, since the deviation between the results is seen more clearly than at other points.

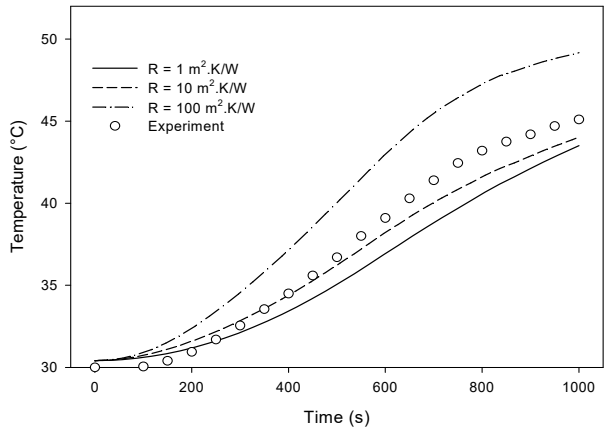

Figure 6. Comparison of FEM and experimental results of the variation of temperature of S-2 point with time for 1, 10, and 100 m^2K/W thermal contact resistance values with h = 5 W/m^2K for all surfaces.

The next step was to repeat the analysis by changing the thermal contact resistance values within the range of 1–100 m^2K/W, until the deviations of the results of the analysis from the experiment were minimized. A total of 500 analyses were run to get the optimum result. The results of the analysis with the final values of the thermal contact resistances and the experimental results are represented in Fig. 7.

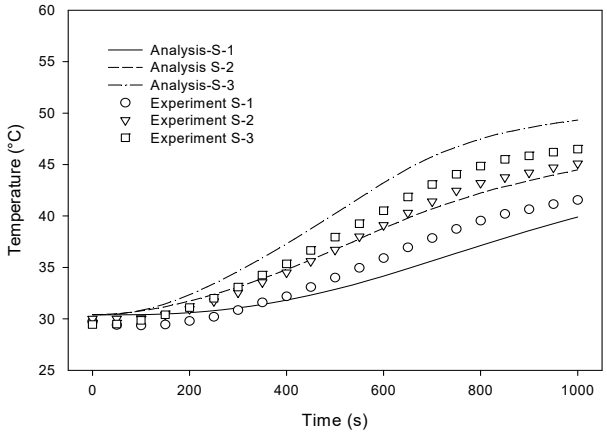

Figure 7. Comparison of FEM and experimental results of the variation of temperature with time for the final values of thermal contact resistances between components and PCB.

Small differences, not exceeding 5°C, have been obtained between the analysis and the experimental results. The main reason for these errors was choosing average constant values for the convective heat transfer coefficients for all surfaces. However, this level of error is acceptable, considering the problem structure.

Determination of Power Deration Rate and Heat Transfer Coefficients

In the second part of the analysis, the power deration rate and the heat transfer coefficients remained as unknown input parameters. The same procedure was followed as in the first part. A physically acceptable range of the power deration value was chosen to make the initial guess.

Power deration rate is generally 10–20%/10 °C for resistor-type components. In order to see the effect of power deration rate on the electronic board temperature, analyses were performed for 10, 15, and 20%/10 °C values of component power deration rate, by keeping the heat transfer coefficient value constant as 5 W/m^2K. The results are shown in Fig. 8, where it is seen that great differences may occur, by up to 10–15 °C, especially for the component temperature.

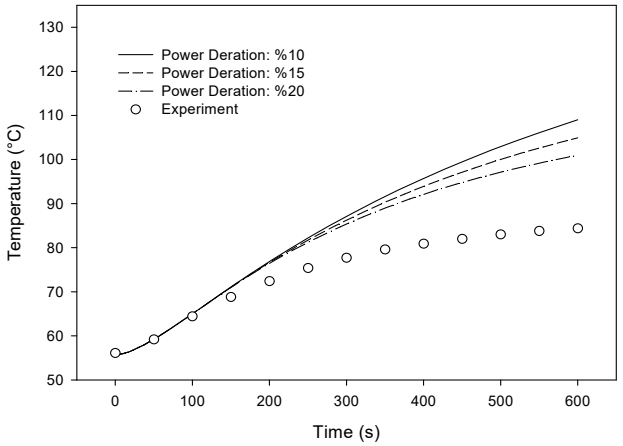

Figure 8. Comparison of FEM and experimental results of the variation of temperature of S-2 point with time for 10%/10 °C, 15%/10 °C and 20%/10 °C component power deration rate values with h = 5 W/m^2K for all surfaces.

The heat transfer between the electronic board and the surrounding air occurs by natural convection, since there was no active cooling element in the experimental setup. The natural convective heat transfer coefficient for air at approximately 1 atm pressure is between 2 and 25 W/m²K (Steinberg, 1991). A sensitivity analysis for the heat transfer coefficients was performed, keeping the component power deration rate at a constant value of 15%/10 °C. The analyses were performed for 5, 15, and 25 W/m²K values of heat transfer coefficients for all surfaces. The results of those analyses are shown in Fig. 9, where it is seen that, for different values of the heat transfer coefficients, differences of up to 20–25°C may be seen, especially for the temperature of the component.

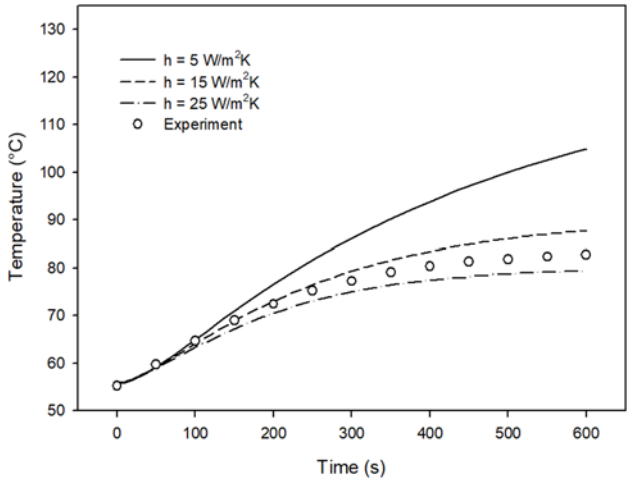

Figure 9. Comparison of FEM and experimental results of the variation of temperature of S-2 point with time for 5, 15, and 25 W/m²K heat transfer coefficient values on all surfaces with component power deration rate is 15%/10 °C.

Considering that the working temperature limits of electronic components are generally around 85 °C, the differences that may rise up to 20–25°C, which were deduced from the analyses, cannot be accepted for a reliable design. This indicates that the component power deration rate and the heat transfer coefficient values have to be determined close to their actual values, to achieve accurate results.

A similar procedure was followed to tune the unknown input parameters, power deration rate, and the heat transfer coefficient values as in the thermal contact resistance values. Shortly, a physically acceptable range of the unknown parameters, and subsequently, the initial values of these parameters were determined. After determining the range of the initial guess and the initial values of the parameters, initial analysis and the iterative analyses were performed. The iteration continued until the results of the analysis and the experiment matched. The component power deration rate and the heat transfer coefficient values were determined in the same tune-up procedure, changing the values concurrently.

The value range of the component power deration was chosen to be 10–20%/10 °C, which is a common range for the component power deration rate. The initial values were chosen to be the mid-value, 15%/10 °C. There are different empirical methods to calculate the heat transfer coefficient on the surfaces of the electronics inside an enclosure. One of them was employed in this study, and it is shown in Eq. (7) (Steinberg, 1991).

$$h = 0.52C\left(\frac{\Delta T}{L}\right)^{0.25} \quad (7)$$

In Eq. (7), h is the heat transfer coefficient (W/m²K), ΔT is the difference between the surface and ambient temperature (°C), and L is the characteristic length of the surface (m). 'C' is a coefficient which depends on the geometry, orientation, and surrounding environment's effects on the surface. This coefficient can only be determined experimentally.

The initial value of the heat transfer coefficient was taken to be 5 W/m²K for all surfaces. The range of the C value was determined as 1–10, considering literature values (Steinberg, 1991). An analysis was performed with the initial values of the component power deration rate and the heat transfer coefficients, where the thermal contact resistance values between the component and the PCB were known. The results of the initial analysis and the experiments are shown in Fig. 10.

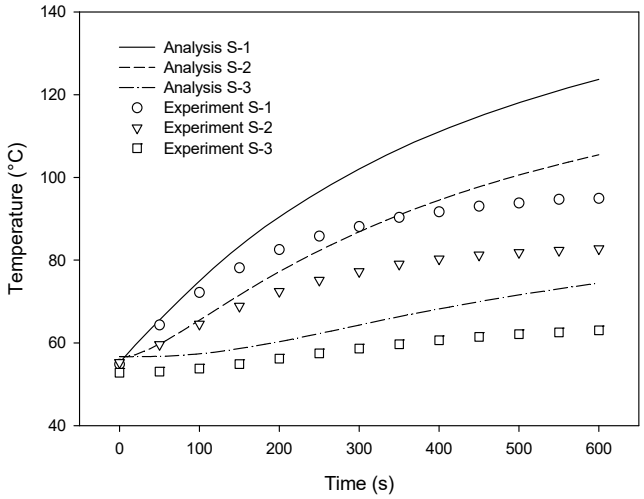

Figure 10. Comparison of FEM and experimental results of the variation of temperature with time for initial values of heat transfer coefficient and component power deration rate (5 W/m²K, %15/10 °C).

Table 2. Corrected 'C' coefficients for surfaces of PCB and components.

Surface	C
Upper Surface of Components	6.8
Long Side Surfaces of Components Facing Each Other	3.9
Long Side Surfaces of Components Facing Outside	3.4
Short Side Surfaces of Components	4.9
Upper Side of PCB Near Components	8.7
Upper Side of PCB Away from Components	2.4
Bottom Side of PCB Near Components	6.8
Bottom Side of PCB Away from Components	5.8

In Fig. 11, it is seen that the maximum difference between the results of the experiments and the analysis is less than 2–3°C. This level of error is quite low for a numerical analysis of this kind of problem. This indicates that a correct analysis model was set up. As long as critical modifications, such as geometry and material properties of the system are not made, the corrected analysis model can be employed to examine the system's thermal behavior under different configurations and boundary conditions. Hence, quick and accurate parametrical analyses can be performed.

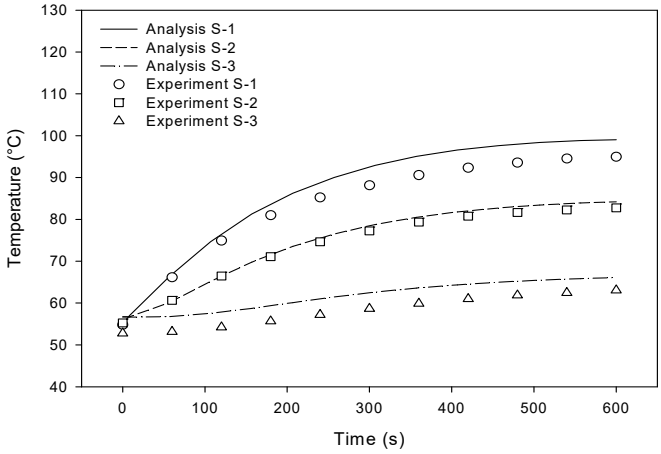

Figure 11. Comparison of FEM and experimental results of the variation of temperature with time for the corrected analysis model.

RESULTS AND DISCUSSION

Parametrical thermal analyses were performed using the corrected analysis model, and the results are presented in this part. The examined parameters were: component power (Q), initial temperature of the whole system ($T_{initial}$), and the heater plate temperature ($T_{heaterplate}$). Realistic values of the parameters were used. For example, 0.5, 1, 2, and 4 mW/mm^3 component power values were used for parametrical analyses, since heat dissipation values are in this order in practical application of electronic components. Initial temperature values were selected as 20, 30, 40, and 50 °C, whereas the effects of the heater plate temperature on the system behavior were examined for 20, 40, 60, and 80 °C, representing the external heat sources' effects.

The main objective of this study was to set up a correct conduction-based FEM analysis model and then to examine the electronic board's thermal behavior for different boundary conditions, using the corrected analysis model. The results of the analyses are presented as the change of the temperature values at some or all of the sensor positions (S-1, S-2, and S-3) during 600 s, and temperature distribution on the upper surfaces of the PCB and components as contour graphs at the final time of 600 s. The results were shown in a way that the effect of one parameter was examined, while the values of the other two parameters were kept constant. The constant values were selected to be the highest and the lowest among all values for which the analyses were performed.

Effect of Q for $T_{initial}$=20°C and $T_{heaterplate}$=20°C

For different values of Q, while $T_{initial}$ = 20 °C and $T_{heater\ plate}$ = 20 °C, the temperature variations of chosen locations on the board and the component are shown in Fig. 12, and the temperature distribution of the upper surface of the board and the components is presented in Fig. 13.

There were two heat sources in the system: the components and the heater plate. The temperature of the S-1 was greatly affected by the component power, while the heater plate temperature had a small effect. On the contrary, the temperature of the S-3 was mainly affected by the heater plate, while it was not much influenced by the component power. S-1 temperature shows a 25–30 °C increase for 4 mW/mm^3 component power, and only a 3–4 °C increase for 0.5 mW/mm^3 component power. S-3 point experienced temperature changes very close to each other for different values of the component power. Since the S-2 point was between S-1 and S-3 in terms of the thermal path, it shows a thermal behavior approximately between the results of S-1 and S-3.

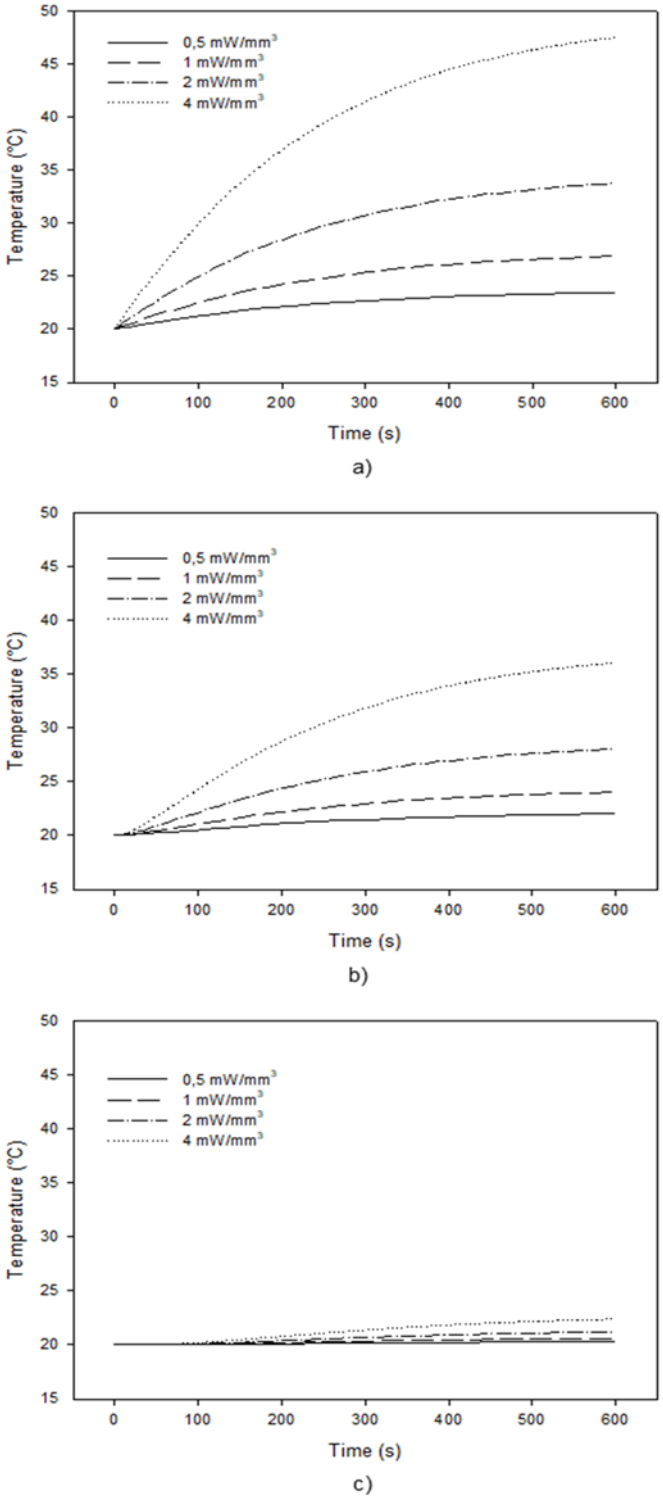

Figure 12. Temperature change with time for different values of component power while $T_{initial}$ = 20 °C and $T_{heater\ plate}$ = 20 °C, a) S-1, b) S-2, c) S-3.

Effect of Q for $T_{initial}$=20°C and $T_{heaterplate}$=80°C

Temperature values of the measurement points for 600 s duration and the temperature contour plot of the upper side of the electronic board and the components are shown in Fig. 14 and Fig. 15, respectively for this boundary condition. For this condition, the heater plate's effect on the sensor points

can be seen, compared with the previous results. According to Fig. 14, S-1 temperature shows a similar increase profile for $T_{initial}$ = 20 °C and $T_{heater\ plate}$ = 80 °C, as is the case for $T_{initial}$ = 20 °C and $T_{heater\ plate}$ = 20 °C, since the heater plate temperature has little effect on S-1 temperature. Temperature of the S-3 increased by about 10–15 °C, when Theater plate = 80 °C for all component power values.

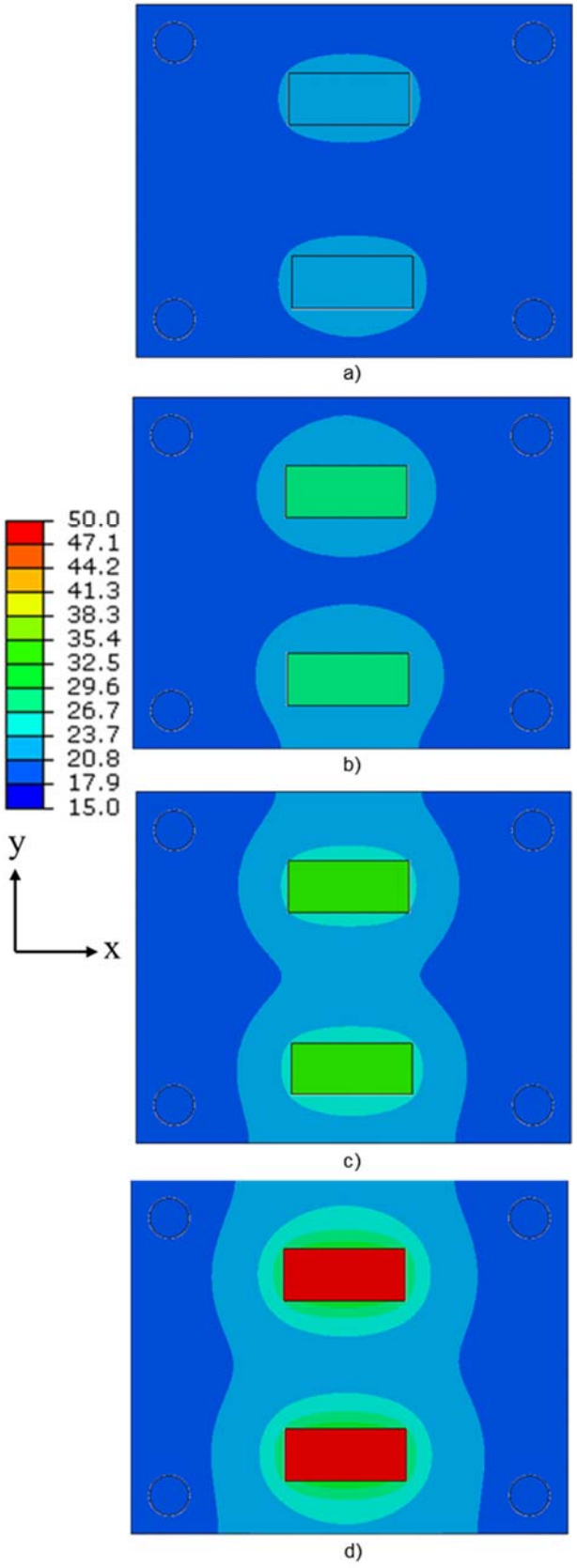

Figure 13. Surface contour plots of temperature at 600 s for $T_{initial}$ = 20 °C and $T_{heater\ plate}$ = 20 °C, a) Q = 0.5 mW/mm³, b) Q = 1 mW/mm³, c) Q = 2 mW/mm³, d) Q = 4 mW/mm³.

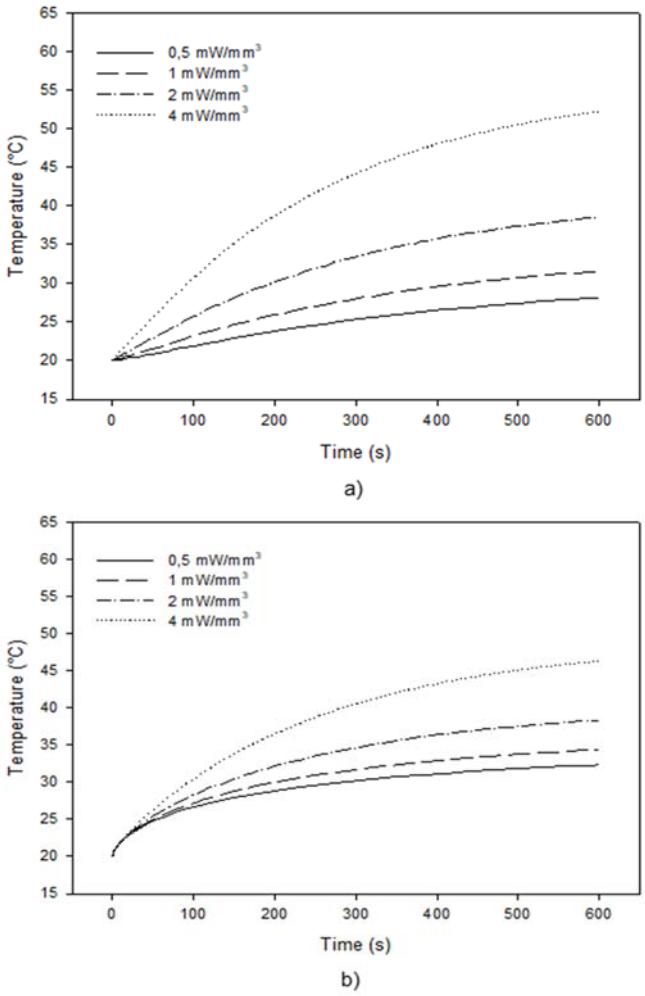

Figure 14. Temperature change with time for different values of component power while $T_{initial}$ = 20 °C and $T_{heaterplate}$ = 80 °C, a) S-1, b) S-2.

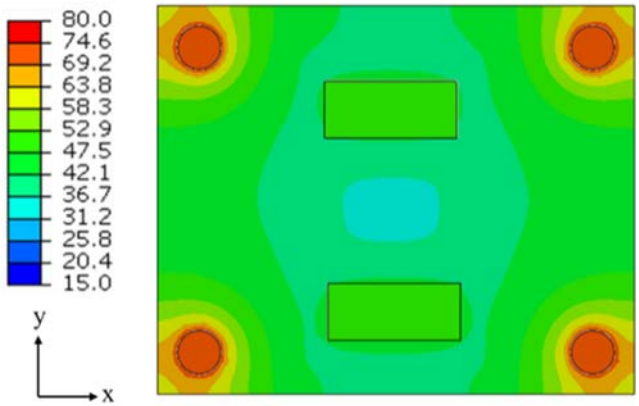

Figure 15. Surface contour plots of temperature at 600 s for $T_{initial}$ = 20 °C and $T_{heater\ plate}$ = 80 °C, Q = 4 mW/mm³.

Effect of $T_{heaterplate}$ for $T_{initial}$=20°C and Q=0.5 mW/mm³

The thermal behavior of the system for different values of the heater plate, while $T_{initial}$ = 20 °C and Q = 0.5 mW/mm³ was examined, and the results are shown in Fig. 16 and Fig. 17, respectively. For this boundary condition, S-1 was not expected to be affected much, since the component power was at its minimum value. On the other hand, S-3 point was expected to heat up quite a lot for $T_{heater\ plate}$ = 80 °C, and not to heat up more than a few degrees for $T_{heater\ plate}$ = 20 °C. In Fig. 16, these expected phenomena can be seen clearly. S-2 again shows a thermal behavior between S-1 and S-3. Moreover, the legs holding the PCB were heated up parallel with the heater plate, since they were in tight contact.

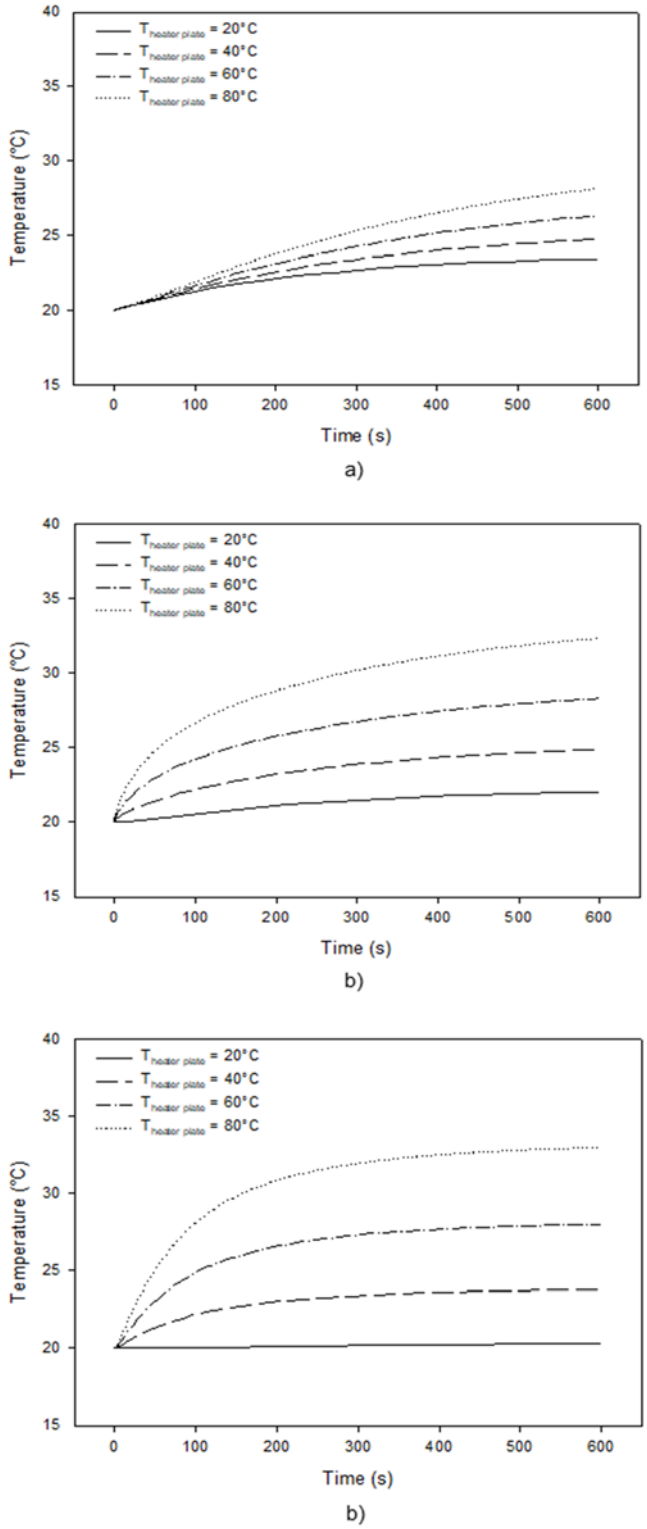

Figure 16. Temperature change with time for different values of $T_{heater\ plate}$ while $T_{initial}$ = 20 °C and Q = 0.5 mW/mm³, a) S-1, b) S-2, c) S-3.

Effect of $T_{heaterplate}$ for $T_{initial}$=20°C and Q=4.0 mW/mm³

For values of $T_{heater\ plate}$ while $T_{initial}$ = 20 °C and Q = 4 mW/mm³, the temperature changes of the measurement points on the board and the component are shown in Fig. 18, and the temperature distribution of the upper surface of the board and the components is presented in Fig. 19. S-3 point represented a temperature change similar to the boundary condition, for which the different values of $T_{heater\ plate}$ were examined, while $T_{initial}$ = 20 °C and Q = 0.5 mW/mm³. However, the temperature values of the S-1 point increased a lot for all values of the heater plate. Again, these results show the effect of the parameters on S-1, S-2, and S-3 points. The PCB legs were affected by the heater plate, similar to the previous results.

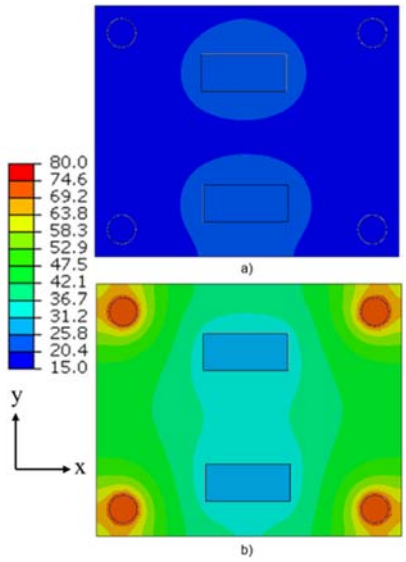

Figure 17. Temperature change with time for different values of $T_{heater\ plate}$ while $T_{initial}$ = 20 °C and Q = 0.5 mW/mm³, a) S-1, b) S-2, c) S-3.

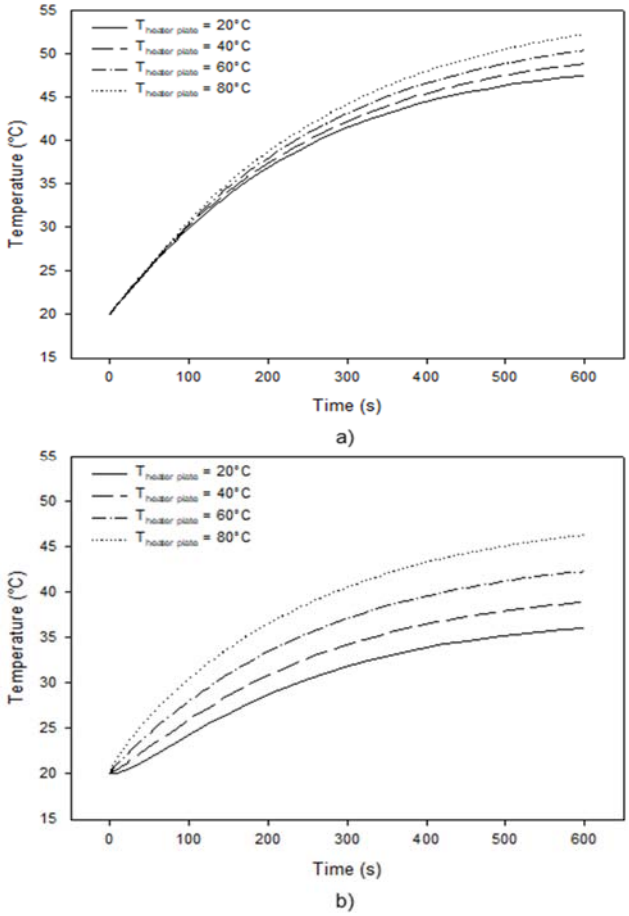

Figure 18. Temperature change with time for different values of $T_{heater\ plate}$ while $T_{initial}$ = 20 °C and Q = 4 mW/mm³, a) S-1, b) S-2.

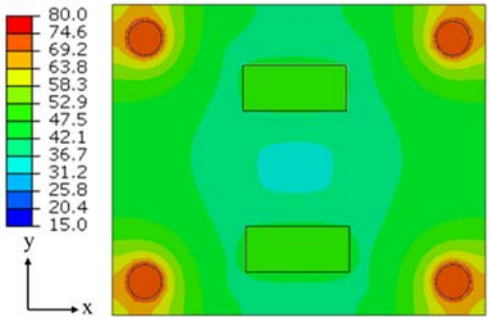

Figure 19. Surface contour plots of temperature at 600 s for $T_{initial}$ = 20 °C and Q = 4 mW/mm³, $T_{heater\ plate}$ = 80 °C.

Effect of $T_{heaterplate}$ for $T_{initial}$=50°C and Q=0.5 mW/mm³

Up to this point, the results of the analyses where $T_{initial}$ = 20 °C, while the other two parameters changed were presented. In Fig. 20 and Fig. 21, results for $T_{initial}$ = 50 °C are presented. 50°C was the maximum value in the interval among which Tinitial was selected. Thermal behaviors of the chosen locations differ for various values of the initial temperature. For the values of the heater plate temperature greater than the initial temperature of the system, temperatures of all three locations increase. However, when the heater plate temperature was lower than the system's initial temperature, the heater plate behaves as a cooler plate. In Fig. 20, especially for Theater plate = 20 °C, the cooling effect of the plate can be seen clearly for all three locations. In Fig. 21, the temperature of the legs also shows this behavior.

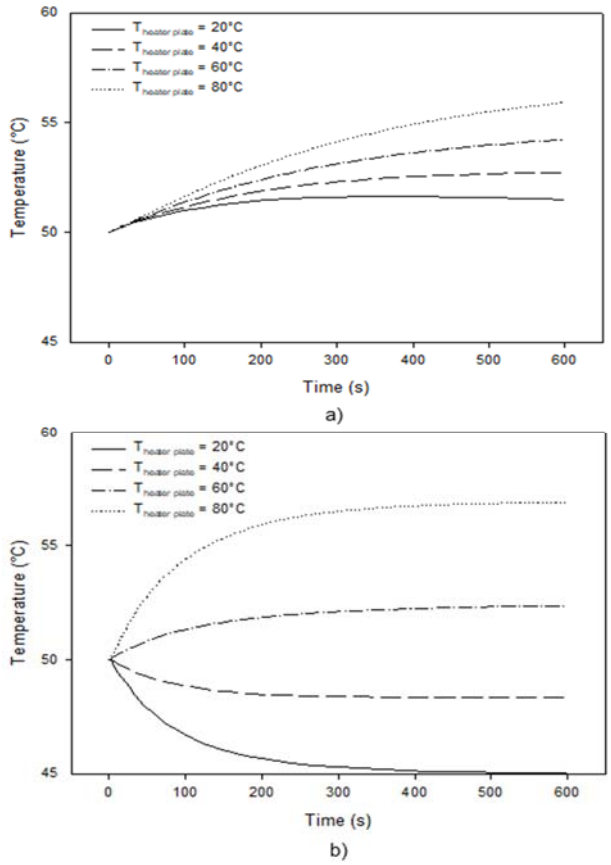

Figure 20. Temperature change with time for different values of $T_{heater\ plate}$ while $T_{initial}$ = 50 °C and Q = 0.5 mW/mm³, a) S-1, b) S-3.

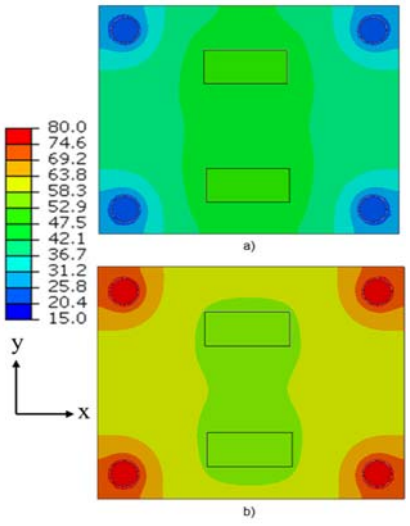

Figure 21. Surface contour plots of temperature at 600 s for $T_{initial}$ = 50 °C and Q = 0.5 mW/mm³, a) $T_{heater\ plate}$ = 20 °C, b) $T_{heater\ plate}$ = 80°C.

Effect of $T_{heaterplate}$ for $T_{initial}$=50°C and Q=4.0 mW/mm³

The results of the analyses performed to see the effect of the heater plate's temperature on the system for $T_{initial}$ = 50 °C and Q = 4 mW/mm³ are shown in Fig. 22 and Fig. 23, respectively. For the S-3 location, the heater plate behaves as a cooler plate for about 200 s. For S-2, this trend was seen for a shorter time, approximately 15–20 s, due to a high heating effect of the components. Temperature of the S-1 point was increasing during the whole time of the analyses for all variations of the heater plate temperature, due to the strong heating effect of the components. The contour plot shown in Fig. 23 is similar to the previous results, in terms of the temperature distribution of legs and region on PCB near legs.

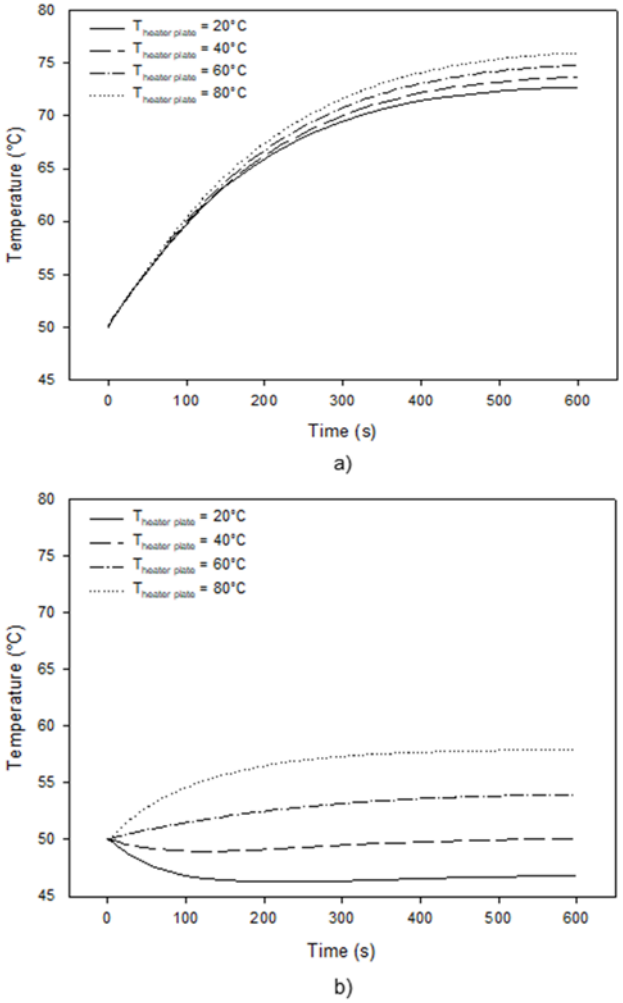

Figure 22. Temperature change with time for different values of $T_{heater\ plate}$ while $T_{initial}$ = 50 °C and Q = 4 mW/mm³, a) S-1, b) S-3.

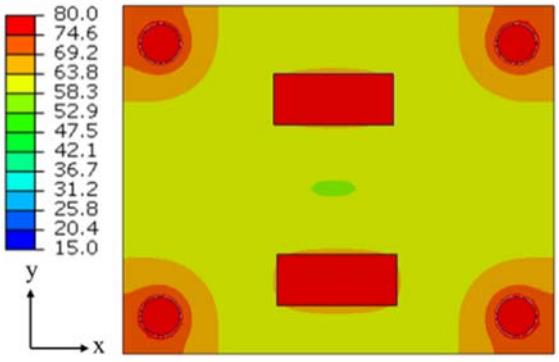

Figure 23. Surface contour plots of temperature at 600 s for $T_{initial}$ = 50 °C and Q = 4 mW/mm³, $T_{heater\ plate}$ = 80 °C.

Effect of $T_{initial}$ for $T_{heaterplate}$=20°C and Q=0.5 mW/mm³

This time, different values of $T_{initial}$ were examined for $T_{heater\ plate}$ = 20 °C and Q = 0.5 mW/mm³, and the results are shown in Fig. 24 and Fig. 25, respectively. Since the component power and the heater plate temperatures were at their minimum values, for all values of the initial temperature, S-1 temperature increased by just a few degrees. It should be noted that the temperature values of the legs were almost the same as in Fig. 25, due to the constant values of the heater plate temperature.

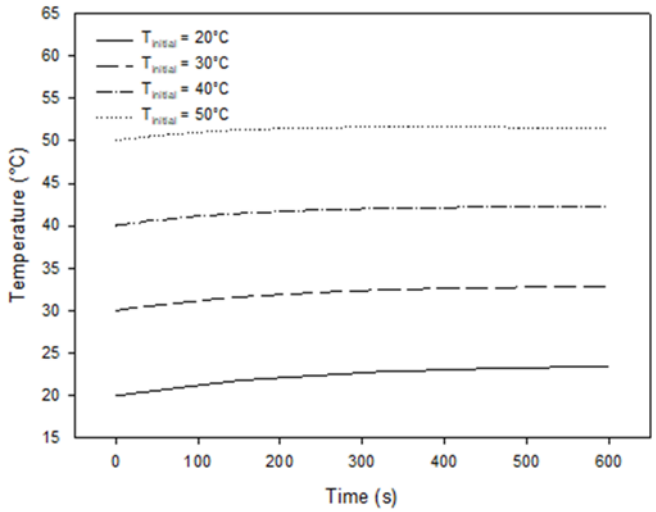

Figure 24. Temperature change with time for different values of $T_{initial}$ while $T_{heater\ plate}$ = 20 °C and Q = 0.5 mW/mm³, S-1.

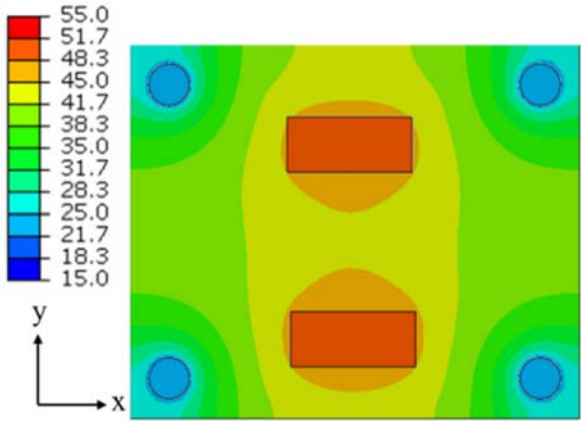

Figure 25. Surface contour plots of temperature at 600 s for $T_{heater\ plate}$ = 20 °C and Q = 0.5 mW/mm³, $T_{initial}$ = 50 °C.

Effect of $T_{initial}$ for $T_{heaterplate}$=20°C and Q=4.0 mW/mm³

Lastly, the results from analyses for different values of the initial temperature while $T_{heater\ plate}$ = 20 °C and Q = 4 mW/mm³ are shown in Fig. 26 and Fig. 27, respectively. As S-3 was not much affected from the component power, the results for location S-3 resemble the previous results of Q = 0.5 mW/mm³. On the other hand, the S-1 point, which was the most affected point from the component power, shows an increase through 600 s, just by temperature shift with various values of initial temperature, since the initial temperature value has no heating effect. Again, the leg temperatures were almost the same because of the heater plate temperature.

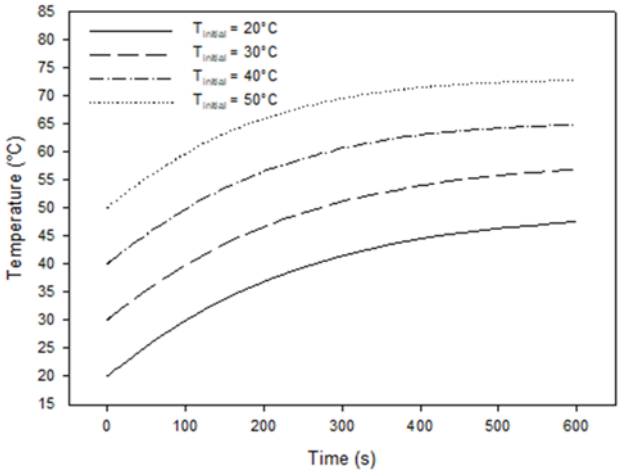

Figure 26. Temperature change with time for different values of $T_{initial}$ while $T_{heater\ plate}$ = 20 °C and Q = 4.0 mW/mm³, S-1.

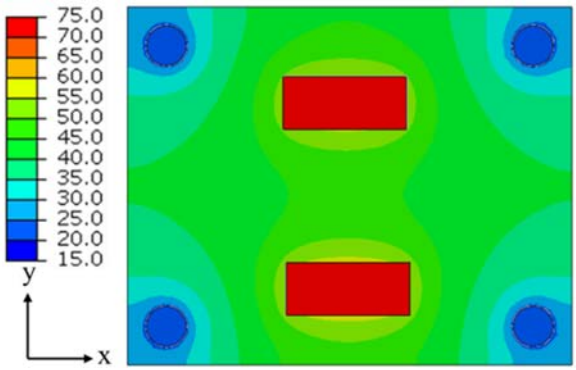

Figure 27. Surface contour plots of temperature at 600 s for $T_{heater\ plate}$ = 20 °C and Q = 4.0 mW/mm³, $T_{initial}$ = 50 °C.

CONCLUSIONS

In this study, a conduction-based FEM analysis model was set up for an electronic board inside an enclosure under transient natural convection conditions. It was aimed to determine the analysis model input parameters which were unknown or uncertain. These were the thermal contact resistance values between the components and the PCB, component power deration rate, and coefficients for calculating the natural convective HTCs at PCB and component surfaces. The unknown input parameters of the analysis were determined using the results of an experimental investigation, which was conducted for the purpose of the correction of the analysis model. The amount of deviations of the results, less than 2-3°C, obtained at the end of the correction process showed that the correct analysis model was set up to perform further analyses for different cases. The findings of the present study could be concluded as follows;

- Preliminary results showed that thermal contact resistance showed best agreement for R=10 m²K/W, where a temperature difference of less than 5°C occurred.
- By using a correlation for the heat transfer coefficient from the literature, it was observed that the deviation of the numerical results compared to experimental results is around 2-3°C.
- It was observed that with the increase in component power for a maximum temperature of around 45.5°C has been obtained under $T_{initial}$ = 20 °C and $T_{heaterplate}$ = 20 °C conditions.

• It was also seen that the heat increase in the heater plate increases the maximum temperature at S-1 to around 50°C with the increase of Q under $T_{initial}$ = 20 °C conditions.
• The effect of heater plate temperature at S-1 is less compared to locations S-2 and S-3 under constant Q and $T_{initial}$ conditions.
• For Q=0.5 mW/mm^3 it was observed that the temperature values become almost constant after around 50 s, whereas for Q=4.0 mW/mm^3 it was seen that the temperature values become constant after around 300 s.

The findings of the present study showed that unless a critical change is made in the system, such as the geometry or the type of the electronic board and the components, material properties, fluid environment, the system under natural convection, or forced convection, the analysis model can be employed for different boundary conditions, with small changes, in order to examine the system's thermal behavior. One of the most important developments which should be considered for future research is to include the ambient temperature as the unknown input parameter and to somehow calculate it in the iterative analyses.

ACKNOWLEDGMENT

The authors would like to thank Roketsan Inc., Ankara, Turkey for funding and technical support.

REFERENCES

Battula, N.K., Daravath, S., Gampa, G.K. (2024). Numerical studies on conjugate convection from discretely heated electronic board. *World Journal of Engineering*, 21(1), 107-114.

Byon, C., Choo, K., Kim, S.J. (2011). Experimental and analytical study on chip hot spot temperature. *International Journal of Heat and Mass Transfer*, 54(9-10), 2066–2072.

Chavan, S., Sathe, A. (2016). Natural convection cooling of electronic enclosure. *International Journal of Trend in Research and Development*, 3(4), 93–97.

Chen, W.H., Cheng, H.C., Shen, H.A. (2003). An effective methodology for thermal characterization of electronic packaging. *IEEE Transactions on Components and Packaging Technologies*, 26(1), 222–232.

Cheng, H.C., Chen, W.H., Cheng, H.F. (2008). Theoretical and experimental characterization of heat dissipation in a board-level microelectronic component. *Applied Thermal Engineering*, 28(5-6), 575-588.

Cheng, H.C., Ciou, W.R., Chen, W.H., Kuo, J.L., Lu, H.C., Wu, R.B. (2013). Heat dissipation analysis and design of a board-level phased-array transmitter module for 60-GHz communication. *Applied Thermal Engineering*, 53(1), 78–88.

Deng, Q.H. (2008). Fluid flow and heat transfer characteristics of natural convection in square cavities due to discrete source–sink pairs. *International Journal of Heat Mass Transfer*, 51(25–26), 5949–5957.

Devellioğlu Y. (2008). *Electronic packaging and environmental test and analysis of an emi shield electronic unit for naval platform*. M.Sc. thesis, Middle East Technical University, Ankara, Turkey.

Ellison, G.N. (2020). *Thermal Computations for Electronics: Conductive, Radiative, and Convective Air Cooling.* (2. Ed.), Boca Raton, FL : CRC Press/Taylor & Francis Group.

Eveloy, V., Rodgers, P., Lohan, J. (2002). *Comparison of numerical predictions and experimental measurements for the transient thermal behavior of a board-mounted electronic component*, ITherm 2002 Eighth Intersociety Conference on Thermal and Thermomechanical Phenomena in Electronic Systems, San Diego, California, USA, 36-45.

Eveloy, V., Rodgers, P. (2005). Prediction of electronic component-board transient conjugate heat transfer. *IEEE Transactions on Components and Packaging Technologies*, 28(4), 817–829.

Gilmore, D.G., Donabedian, M. (2003). *Spacecraft Thermal Control Handbook*. Reston, Virginia: American Institute of Aeronautics and Astronautics.

Han, C.K., Jung, H. (2017). *A study on thermal behavior prediction for automotive electronics unit based on CFD*. 23rd International Workshop on Thermal Investigations of ICs and Systems (THERMINIC), Amsterdam, Holland, 1-4.

Holman, J.P. (1994). *Experimental Methods for Engineers.* (Sixth Ed.), McGraw-Hill, New York.

Joshy, S., Jellesen, M., Ambat, R. (2017). *Effect of interior geometry on local climate inside an electronic device enclosure*. 16th IEEE Intersociety Conference on Thermal and Thermomechanical Phenomena in Electronic Systems (ITherm), Orlando, Florida, USA, 779-783.

Khatamifar, M., Lin, W., Armfield, S.W., Holmes, D., Kirkpatrick, M.P. (2017). Conjugate natural convection heat transfer in a partitioned differentially-heated square cavity. *International Communications in Heat and Mass Transfer*, 81, 92–103.

Lim, C.H., Abdullah, M.Z., Aziz, I.A., Khor, C.Y., Aziz, M.S.A. (2021). Optimization of flexible printed circuit board's cooling with air flow and thermal effects using response surface methodology. *Microelectronics International*, 38(4), 182-205.

Lira, E., Greenlee, C. (2007) *Thermal analysis and testing of missile avionics systems*, AIAA Thermophysics Conference, Miami, Florida, USA.

Nogueira, R.M., Martins, M.A., Ampessan F. (2011). Natural convection in rectangular cavities with different aspect ratios. *Revista De Engenharia Térmica*, 10(1-2), 44-49.

Ocak M. (2010). *Conduction-based compact thermal modeling for thermal analysis of electronic components.* M.Sc. thesis, Middle East Technical University, Ankara, Turkey.

Otaki, D., Nonaka, H., Yamada, N. (2022). Thermal design optimization of electronic circuit board layout with transient heating chips by using Bayesian optimization and

thermal network model. *International Journal of Heat and Mass Transfer*, 184, 122263.

Pang Y.F. (2005). *Assessment of thermal behavior and development of thermal design guidelines for integrated power electronics modules*. Ph.D. dissertation, Virginia Polytechnic Institute and State University, Blacksburg, Virginia, USA.

Rakshith, B.L., Asirvatham, L.G., Angeline, A.A., Manova, S., Bose, J.R., Raj, J.P.S., Mahian, O., Wongwises, S. (2022). Cooling of high heat flux miniaturized electronic devices using thermal ground plane: An overwiev. *Renewable and Sustainable Energy Reviews*, 170, 112956.

Rodgers, P., Eveloy, V., Lohan, J., Fager, C.M., Tiilikka, P., Rantala, J. (1999). *Experimental validation of numerical heat transfer predictions for single and multi-component printed circuit boards in natural convection environments*. Fifteenth Annual IEEE Semiconductor Thermal Measurement and Management Symposium, San Diego, California, USA, 54-64.

Rosten, H.I., Parry, J.D., Addison, J.S., Viswanath, R., Davies, M., Fitzgerald, E. (1995). *Development, validation and application of a thermal model of a plastic quad flat pack*, 45th Electronic Components and Technology Conference, Las Vegas, Nevada, USA, 1140-1151.

Stancato, F., dos Santos, L.C., Pustelnik, M. (2017). Electronic package cooling analysis in an aircraft using CFD. *SAE Technical Paper Series*, 1.

Steinberg, D.S. (1991). *Cooling Techniques for Electronic Equipment,* (2nd ed.), Nashville, TN: John Wiley & Sons.

Taliyan, S.S., Sarkar, S., Biswas, B.B., Kumar, M. (2010) *Finite element based thermal analysis of sealed electronic rack and validation*, 2nd International Conference on Reliability, Safety and Hazard - Risk-Based Technologies and Physics-of-Failure Methods (ICRESH), Mumbai, India, 443-447.

Wang, Z., Zheng, S., Xu, S., Dai, Y. (2024). Investigation on the thermal and hydrodynamic performances of a micro-pin fin array heat sink for cooling a multi-chip printed circuit boards. *Applied Thermal Engineering*, 239, 122178.

Xu, G. (2017). *Multi-core server processors thermal analysis.* 16th IEEE Intersociety Conference on Thermal and Thermomechanical Phenomena in Electronic Systems (ITherm), Orlando, Florida, USA, 416-421.

Zahn, B.A., Stout, R.P. (2002). *Evaluation of isothermal and isoflux natural convection coefficient correlations for utilization in electronic package level thermal analysis*. Thirteenth Annual IEEE Semiconductor Thermal Measurement and Management Symposium, Austin, Texas, USA.

Zaman, F.S., Turja, T.S., Molla, M.M. (2013). Buoyancy driven natural convection flow in an enclosure with two discrete heating from below. *Procedia Engineering*, 56, 104–111.